Submitted to Physical Review
March, 1975

ANL/HEP 7427 Rev.
FERMILAB-PUB-75-119-E

A 141A

Study of the Reaction $p + p \rightarrow \Delta^{++}(1236) + X^{o}$ at 205 GeV/c

S.J. BARISH, M. DERRICK, B. MUSGRAVE, and P. SCHULTZ
Argonne National Laboratory, Argonne, Illinois 60439*

and

J. WHITMORE+
Fermi National Accelerator Laboratory, Batavia, Illinois 60510‡

and

R. ENGELMANN, T. KAFKA, and M. PRATAP§
State University of New York, Stony Brook, New York 11790x

and

R.D. FIELD
California Institute of Technology, Pasadena, California 91109*

We have studied inclusive $\Delta^{++}(1236)$ production for $|t_{p\Delta}| < 1.0\ (\text{GeV/c})^2$ in a 50,000 picture exposure of the 30-inch hydrogen bubble chamber to a 205 GeV/c proton beam. The inclusive Δ^{++} cross section for one CM hemisphere is (1.30 ± 0.14) mb. The mean charged multiplicity of the system recoiling off the Δ^{++} is in agreement with that for laboratory $\pi^- p$ interactions at the same center of mass energy. The inclusive Δ^{++} production is com-

---

*Work supported by the U.S. Atomic Energy Commission

+Present Address: Michigan State University, East Lansing, Michigan 48823.

‡Operated by Universities Research Association, Inc. under contract with the U.S. Atomic Energy Commission.

§Present Address: University of Mons, 7000 Mons, Belgium

xWork supported by the National Science Foundation

pared to inclusive Λ^o and proton production in the same experiment. The connection between Δ^{++} production and diffraction is discussed. We find that not all Δ^{++} come from the decay of a diffractively-produced state. The P_T^2 distribution for the Δ^{++} has slope of (10.5 ± 0.9) $(GeV/c)^{-2}$ for $P_T^2 \lesssim 0.2$ $(GeV/c)^2$. This slope, together with the decay angular distribution of the Δ^{++} at small momentum transfer, suggests a strong pion exchange contribution to the inclusive process. We compare the data to the expectation of a Triple Regge Model with ρ and π exchange contributions.

I. Introduction

There has been an increasing interest in diffractive phenomena in recent years as high energy results from the CERN Intersecting Storage Rings (ISR) and the Fermi National Accelerator Laboratory (FNAL) have become available. The data show prominent low mass peaks in the missing masses recoiling from either of the incident particles;[1] alternatively one observes a peak in the Feynman x variable near $x = \pm 1$ for one of the scattered particles. This is interpreted as diffractive excitation of one of the incident hadrons into a low mass system ($\lesssim 5$ GeV). The cross section for diffractive excitation of a single particle is about 2 to 3 mb and is independent of beam energy in the several hundred GeV region. Bubble chamber experiments show that the contributions to the low mass peak come predominantly from the 2-, 4- and 6-prong

events for both $\pi^{\pm}$p and for pp interactions.

In addition to the diffractive phenomena, the high energy experiments have also established that the single particle spectra for the stable final state particles show an approximate scaling behavior.[2] This behavior already sets in at large x values for pions in the tens of GeV energy region. However, scaling does not hold for the heavier stable particles in the central region even at the highest energies studied.

We have extended these investigations of high energy interactions to an unstable final state particle system by studying inclusive $\Delta^{++}(1236)$ production in 205 GeV/c pp collisions using pictures from the 30-inch bubble chamber exposed at FNAL. In particular, we examine the relationship between Δ^{++} production and diffraction. Results similar to ours were first obtained by the FNAL-UCLA collaboration[3] using the same bubble chamber exposed to 303 GeV/c proton beam. The present paper reports a much larger sample of data at a beam momentum of 205 GeV/c.

II. Experimental Method

A double scan was made of 50,000 pictures of 205 GeV/c proton-proton interactions to record all events; the overall scanning efficiency was measured to be 96 ± 2%.[4] For this study we selected all events having two or more tracks with laboratory momentum < 1.5 GeV/c, one of which could be identified as a proton track.

After the measurement of these slow particle tracks and spatial recon-

struction using the program TVGP, they were examined by a physicist and classified as π^+, p or π^- on the basis of curvature and bubble density. This separation was essentially unambiguous after restricting the laboratory momentum to be less than 1.4 GeV/c. Furthermore, any bias coming from the difficulty of separating the π^+ and proton interpretations at the higher momenta will only affect the small interval of Δ breakup angles in which the proton follows exactly along the Δ line of flight. Table I summarizes the event sample resulting after three measurement passes, broken down according to the overall event topology. We show in the table both the number of events found and the final numbers weighted to account for the few events that failed reconstruction. The normalization of the data reported in this paper is 4.66 μb/event, which may be directly applied to the weighted events to obtain cross sections.

The cut at 1.4 GeV/c laboratory momentum for unambiguous π^+/p separation by bubble density allows essentially full acceptance for all Δ breakup angles provided that the four momentum transfer between the target proton and the Δ, $|t_{p\Delta}|$, is less than 1 $(\text{GeV/c})^2$. This corresponds to a Δ laboratory momentum of 1.33 GeV/c.

Fig. 1 shows the kinematic situation on a P_T^2 vs. x graph where $x = \frac{2P^*_L}{\sqrt{s}}$; here, P^*_L is the Δ longitudonal CM momentum and $s = 386\ \text{GeV}^2$ is the square of the CM energy. The area below the dotted line is the kinematic region of the experiment, $|t_{p\Delta}| < 1\ (\text{GeV/c})^2$. Also shown on the axis are the missing mass values corresponding to the given x values calculated from the relation $M^2 = s(1-x)$, which is a good approximation in this case. For comparison we show

as dots the protons from the decay of the Δ^{++} after the $|t_{p\Delta}| < 1$ (GeV/c)^2 cut has been applied.

Table II shows how the sample is distributed according to the number of low-momentum pions associated with the identified proton. We see that the chance of finding an extra low-momentum pion is small; the number of events decreases by about a factor of 5 for each additional pion. The number of negative pions is about three quarters of the number of positive pions. We also give, for comparison, the corresponding data at 303 GeV/c.[3]

III. Results

A. Δ Cross Sections

Fig. 2 shows the $p\pi^+$ and $p\pi^-$ mass distributions. A clear Δ^{++} signal is seen in the $p\pi^+$ combinations over a substantial background. There is little sign of a Δ^0 enhancement in the $p\pi^-$ mass plot of Fig. 2(b). The shaded histograms correspond to the $|t_{p,\,p\pi^+}| < 1$ (GeV/c)^2 cut which results in an unbiased selection of events. One sees that the $p\pi^-$ shaded distribution is similar to the background under the Δ^{++} peak of Fig. 2(a).

A measurement of the inclusive Δ^{++} cross section is a somewhat arbitrary procedure since the Δ^{++} is a wide resonance and one must take account of the background under the peak. Defining a Δ as any $p\pi$ combination with mass ≤ 1.5 GeV above the hand-drawn background curves shown in Fig. 2, we measure, for $|t_{p\Delta}| < 1$ (GeV/c)^2, the inclusive cross sections,

$$p + p \rightarrow \Delta^{++} + X^0 , \qquad \sigma = 1.30 \pm 0.14\,\text{mb} \tag{1}$$

$$p + p \rightarrow \Delta^{o} + X^{++} \quad , \qquad \sigma = 0.33 \pm 0.36 \text{ mb} \tag{2}$$

with Δ^{o} corrected for the $n\pi^{o}$ decay mode. These and subsequent cross sections are quoted for one CM hemisphere. Only 6% of the events have more than one $p\pi^{+}$ mass combination ≤ 1.5 GeV for $|t_{p\Delta}| < 1$ $(\text{GeV/c})^2$. Since such a background subtraction is somewhat arbitrary, we also quote in Table III the cross section for reaction (1), defining the Δ^{++} as any $p\pi^{+}$ mass combination in the interval $1.12 \leq M(\pi p) \leq 1.32$ GeV. This selection gives a much larger cross section. We note that using the background subtracted results, the ratio of Δ^{++} to Δ^{o} inclusive cross sections is in reasonable agreement with the 9/1 ratio expected for I = 1 exchange. Our measured cross section of 1.30 ± 0.14 mb, when compared to the total inelastic cross section of 32.1 ± 1.1 mb, implies that 8% of the inelastic events contain a Δ^{++}. In the same experiment it was found that 10.3 ± 1.1% of the inelastic events contained a Λ^{o}.[5] Fig. 3 illustrates the topological dependence of the Δ^{++} production with $|t_{p\Delta}| < 1$ $(\text{GeV/c})^2$. There are very few events in the 2-prong topology (Table I), but clear peaks are visible in the 4- and 6- prong topologies, and a small signal appears in the 8- and $\geq$ 10- prong events.[6] We have used the hand-drawn background curves shown to estimate the topological dependence of the overall Δ^{++} production. The results are summarized in Table IV.

B. Comparison of Cross Section with Results at Other Energies

Inclusive Δ^{++} production has also been studied at other energies, and we show in Fig. 4 the inclusive $p\pi^{+}$ mass spectrum with the $|t_{p,(p\pi^{+})}| <$

1 $(GeV/c)^2$ selection for data at 12, 24, 69, 205, and 303 GeV/c.[7] In each case, one sees a clear Δ^{++} signal although the shape of the distribution varies somewhat from experiment to experiment. Using the hand-drawn backgrounds shown and using all the events above the curves in the Δ region (1.12 to 1.32 GeV) give the cross section values plotted in Fig. 5.[8] The errors are statistical only except for the 12 and 24 GeV/c experiments. For this high statistics data we have arbitrarily assigned a 5% error in an attempt to account for the uncertainty in our background estimate. The cross section falls by about a factor of two in going from 12 to 69 GeV/c and then levels out at an approximately constant value of 1.5 mb. This constancy of the Δ^{++} inclusive cross section at high energy has also been noted by the Rochester-Michigan group.[8] However, the data are also consistent with the $P_{Lab}^{-0.29 \pm 0.03}$ variation shown, particularly considering the possible systematic errors coming from comparing results from different experiments and the arbitrary nature of the background estimation. It is interesting to note that the OPE triple Regge models discussed later in Section G would predict very little dependence of the inclusive cross section on beam momentum above about 50 GeV/c.[9]

C. Properties of the $p\pi^+\pi^-$ System

The $p\pi^+\pi^-$ mass distribution of Fig. 6(a) shows a general low mass peaking, but no clear structure except possibly in the 1700 MeV region. One must remember that this distribution is biased as we have selected all laboratory momenta to be smaller than 1.4 GeV/c. Fig. 6(b) shows the $\Delta^{++}\pi^-$ mass dis-

tribution with a Δ^{++} defined as any $p\pi^+$ mass combination in the range 1.12 to 1.32 GeV. In Fig. 6(c) we show the $\pi^+\pi^-$ mass distribution which peaks strongly at low masses with only a suggestion of ρ production.

D. Comparison with Inclusive Proton Production

Experiments studying the inclusive proton production reaction

$$p + p \rightarrow p + X^+ \tag{3}$$

find[10] a striking low mass peak in the distribution of the missing mass (M_X^2) corresponding to the system X^+ recoiling from the proton. This diffractive excitation of the incident proton can be understood in terms of an exchange process depicted by the diagram shown in Fig. 7(a).

We may compare data from the present study of inclusive Δ^{++} production with these results. However, Pomeron exchange is forbidden in the inclusive Δ^{++} reaction because of the charge exchange at the lower vertex, and we assume I = 1 exchange (π, ρ...) will be the dominant contributions, as shown in Fig. 7(c). The distribution of the missing mass squared of the system X is shown in Fig. 8 for reactions (1) and (3). The dominant low mass peak seen in the inclusive proton data is completely absent for the system recoiling from a Δ^{++}. We estimate that no more than 15 ± 10 events corresponding to a cross section of 70 ± 50 μb could be in the low mass peak in the Δ^{++} reaction, whereas the diffractive cross section for the proton reaction at 205 GeV/c is 2.6 ± 0.3 mb.[10]

A further interesting result of the inclusive proton studies is that the charged multiplicity distribution of the system X^+ in reaction (3) follows that

for the reaction

$$p + p \rightarrow \text{anything} \tag{4}$$

at an equivalent center of mass energy.[10, 11]

Since we expect pion exchange to be an important contribution to the inclusive Δ^{++} production, we compare in Fig. 9 (a) the mean charged multiplicity of X^{o} from reaction (1) with that from the reaction

$$\pi^{-}p \rightarrow \text{anything} \tag{5}$$

at equivalent center of mass energies. The data for reaction (5), including the elastic scattering contribution, are shown as the line and agree reasonably well with the data from reaction (1). However, whether this agreement should be taken as evidence that off-mass-shell $\pi^{-}p$ scattering behaves much like real $\pi^{-}p$ collisions is not clear. For example, one can consider the analogous process (2) for Δ^{o} production. As shown above, there is very little Δ^{o} produced in this experiment. However, if we make the same selection on $M(p\pi^{-})$ (i.e. 1.12 to 1.32 GeV) and compute the average multiplicity recoiling off the "Δ^{o}" we find the data shown in Fig. 9 (b). Similarly, we compare these results to $\pi^{+}p$ scattering:

$$\pi^{+}p \rightarrow \text{anything} \tag{6}$$

again at equivalent CM energies. The agreement is almost as good as in Fig. 9 (a) even though the diagram corresponding to Fig. 7 (b) for Δ^{o} production is unlikely to occur in the experiment (no observable Δ^{o} signal in Fig. 2 (b)).

In conclusion, it would appear that the agreement observed in Fig. 9 for

reactions (1) and (2) and in Ref. 10 and 11 for reaction (3) seems to be a universal effect and may have no direct connection with the concept of a simple, single-particle-exchange process. This conclusion is strengthened by the data shown in Fig. 10 for the average charged multiplicity, $< n_c >$, for p, Λ^o, π^-, K_s^o, Δ^{++} and "Δ^o" as a function of x. These data are from pp interactions at 19 GeV/c and from the present experiment at 205 GeV/c. Since $x \sim M^2$ and since all of the data seem in quite good agreement, these results are certainly in accord with the above conclusion.

E. Relationship Between Δ^{++} Production and Diffraction

We now turn to a more detailed discussion of the connection between the Δ^{++} production and diffraction. From a comparison of inclusive Δ^{++} production in $\pi^- p$ interactions at 15 GeV/c with that in pp interactions at 303 GeV/c, Brick et al concluded that all the Δ^{++} result from the decay of a diffractively-produced state.[12] A further conclusion of this analysis is that attempts to describe the inclusive Δ^{++} data for reaction (1) in terms of a one-pion-exchange (OPE) Triple-Regge Model will be incorrect.

There is clearly a connection between Δ^{++} production and diffraction which we now explore in more detail. Since from studies of reaction (3) it is known that diffraction dissociation of the proton is predominantly into low multiplicity final states, we have isolated Δ^{++} production as a function of event topology as previously discussed. Table IV lists these cross sections which are obtained from the $p\pi^+$ mass plots for the individual topologies shown in Fig. 2. They are

defined as the number of events above the hand drawn backgrounds shown. With our limited number of events, no unambiguous Δ^{++} signal is seen for topologies with ≥ 8 prongs, although some low mass peaking is evident.

In Fig. 11 we compare the total charged multiplicity distribution of the Δ^{++} events with both the overall charged multiplicity and the charged multiplicity coming from the diffractive events of reaction (3). It is clear the Δ^{++} multiplicity lies between the other two, implying that there is not a complete congruence between Δ^{++} production and diffraction.

From Table IV, we see that not all diffractive four-prong events contain a Δ^{++}. In a study of the complete 4-prong events [13] we found that only two-thirds of the Δ^{++} in this topology appear to be fragments of diffractively-produced states. An analysis of the 6-prong events from this experiment [14] shows that of the 0.38 mb of diffraction, only 0.10 ± 0.03 mb corresponds to events containing a Δ^{++}, whereas the 6 prong contribution to the inclusive Δ^{++} production has a cross section of 0.49 ± 0.08 mb. We conclude then that although Δ^{++} as the decay products of a diffractively-produced higher mass system is important, not all Δ^{++} come from this source contrary to the conclusion of the MIT group. [12] In fact, on elementary considerations, one would not expect produced Δ^{++}'s to come completely from diffractive events any more than, for example, final state neutrons.

F. Comparison of the Production Characteristics of the Proton, Λ°, and $\Delta^{++}(1236)$

Any comparison of the inclusive production of the heavy particles such as

proton, Λ^o and Δ^{++} must reckon with the dominant leading particle effect in the proton case where it recoils from a diffractively produced state, which as we have seen (Fig. 8) does not occur for the Δ^{++} case. Nor does it for the Λ^o production.[5] In order to make this comparison, we have removed this leading particle contribution to the proton production data in two ways; first we use only those protons which are associated with one or more identified slow pions, while the second method uses only those events in which the system X^+ recoiling from the identified proton has $M_X^2 \geq 40$ GeV^2, i.e. outside the diffraction region.

In Fig. 12(a), we show the distribution in CM rapidity, $y^* = 1/2 \log \frac{E^* + P_L^*}{E^* - P_L^*}$ for the inclusive proton sample. The corresponding distributions for the two samples in which the leading proton has been removed are shown in Fig. 11 (b) and (d). The corresponding distributions for the Δ^{++} and Λ^o are shown in Fig. 11 (c), (e) respectively where in (e) we show as the dotted histogram the $\bar{\Lambda}^o$ events. These latter events occur for $y^* \approx 0$ as expected for $\Lambda\bar{\Lambda}$ pair production. One notes a striking similarity between the y^* distributions for p, Λ and Δ^{++} in that they each have a prominent peak at $y^* \approx -2.5$. However, one should recognize that our selection criteria preclude our observing either p or Δ^{++} for $y^* \gtrsim -2.0$.

The inclusive distributions in P_T^2 for each of the three particles are compared in Fig. 13, and one sees qualitatively similar features. None of the distributions can be described using a single exponential, and in each case there is

evidence for a break in slope at $P_T^2 \sim 0.3$ (GeV/c)^2. However, the slope of the distribution for $P_T^2 \lesssim 0.3$ (GeV/c)^2 is different in each case with the Δ^{++} having the largest and the Λ^0 the smallest slope.

G. Triple Regge Analysis

It has been suggested that in inclusive charge exchange processes such as reaction (1), the OPE process could provide a large contribution to the inclusive cross section.[15-17] In terms of the variables (x, P_T) for the Δ^{++}, the OPE contribution will be important for $x \lesssim -0.8$ and small P_T. In particular, a very sharp rise is predicted in the x spectrum, away from $x \sim -1.0$. Alternatively, one should expect the missing-mass squared (MM^2) distribution to fall rapidly as threshold is approached. In terms of a triple Regge model, the process should be described by the diagrams of Fig. 7 (b) and (d). However, in addition to π exchange, one can also anticipate that other I = 1 states, such as the ρ, will contribute. In a comprehensive triple Regge analysis of the inclusive proton reaction (3), Field and Fox[18] concluded that inclusion of the $\pi\pi\mathbb{P}$ and $\pi\pi R$ terms was very important in determining the magnitude of the $RR\mathbb{P}$ term. Based on this analysis, predictions were made for the inclusive charge exchange reaction

$$p + n \rightarrow p + X \qquad (6)$$

where the $\pi\pi\mathbb{P}$ and $\pi\pi R$ terms can be expected to be even more important. Preliminary FNAL data for reaction (6) at $s = 110$ GeV^2 and fixed t values of $-t = 0.16$ and 0.4 (GeV/c)^2 showed very good agreement with the predicted

Born $\pi\pi P + \pi\pi R$ terms.[18] Note that in general the Born $\pi\pi P + \pi\pi R$ terms could be modified by off-shell effects and absorptive corrections analogous to those found in two-body π-exchange processes. The analysis of Field and Fox considered these corrections by multiplying the Born term by a factor exp $(a(t - m_\pi^2))$. They found the data for reactions (3) and (6) to be relatively insensitive to the choice of a and for simplicity took $a \approx 0$. Predictions analogous to those made for reaction (6) can also be made for our inclusive Δ^{++} production.

We first examine to what extent our data suggest a dominant OPE contribution. The distribution in $t' = t - t_{min}$ for the inclusive Δ^{++} reaction is shown in Fig. 14. There seems to be a change in slope of the distribution at $|t'| \sim 0.3$ $(GeV/c)^2$. Using the functional form $d\sigma/dt' = A \exp Bt'$, we obtain $B = 8.6 \pm 0.9$ $(GeV/c)^{-2}$ for $0.02 < |t'| < 0.27$ $(GeV/c)^2$. This is characteristic of reactions mediated by pion exchange. The x distribution of the Δ^{++} (Fig. 15 (a)) shows a broad maximum at $x \sim -0.85$ with a fairly rapid fall-off as $x \to -1.0$, also qualitatively expected for OPE. By requiring small t' or P_T^2, this characteristic appropriate to OPE should be enhanced. However, the data show no significant change, as seen in Fig. 15 (b). Fig. 15 (b) also shows the contributions of the unmodified $\pi\pi P + \pi\pi R$ Born term and triple Regge $\rho\rho P + A_2A_2P$ terms predicted from factorization using the analysis of Field and Fox on inclusive proton production. The Born term prediction for the $\pi\pi P + \pi\pi R$ triple Regge term is substantially larger than indicated by the data.[19] Thus if one is to maintain the triple Regge interpretation one must modify the OPE Born term

contribution through off-mass-shell and/or absorptive corrections. This is not surprising since sizeable absorptive corrections to OPE are required in two-body processes. Fig. 16 shows a much improved fit to the $p + p \rightarrow \Delta^{++} + X^{o}$ data, where the π Born term has been modified by the factor $\exp(6t_{p\Delta})$.

The decay angular distribution of the Δ^{++} in the Gottfried-Jackson (t-channel) frame can be expressed as:

$$W(\theta, \phi) = \frac{3}{4\pi} \{ \sin^2\theta \, \rho_{33} + (\cos^2\theta + 1/3) \, \rho_{11} - \frac{2}{\sqrt{3}} \sin 2\theta \cos\phi \, \mathrm{Re}\, \rho_{31} - \frac{2}{\sqrt{3}} \sin^2\theta \cos 2\phi \, \mathrm{Re}\, \rho_{3,-1} \} \quad . \tag{7}$$

In Fig. 17 (a, b) we show the distributions of $\cos\theta$ and ϕ in the t-channel coordinate system, requiring $P_T^2 \leq 0.1$ (GeV/c)^2 for the Δ^{++}. The $\cos\theta$ distribution shows a slight asymmetry due to the non-Δ^{++} background. The distribution in the Treiman - Yang angle, ϕ, is consistent with isotropy. For comparison, we show in Fig. 17 (c, d) the corresponding distributions with identical mass, t, and P_T^2 cuts, for the $p\pi^-$ system. Here the asymmetry in $\cos\theta$ is much more pronounced. The density matrix elements were determined using moments, e.g.

$$\langle Y_2^o \rangle = \frac{2}{\sqrt{2\pi}} \langle \rho_{11} - \rho_{33} \rangle \, ,$$

with the results shown in Table V. For pure, unabsorbed OPE, the value $\rho_{11} = 0.5$ is expected. Our result would then allow quite a large $\rho(A_2)$ contribution, although we note that the results at 303 GeV/c are in better agreement with pure pion exchange.[3] Absorptive corrections to the one-pion exchange could be impor-

tant, however, it is not very clear how to incorporate such effects. One procedure due to Gotsman[15] gives the values $\rho_{11} = 0.38$, $\mathrm{Re}\,\rho_{31} = 0.06$ and $\mathrm{Re}\,\rho_{3-1} = 0.03$ in good agreement with our results.

IV. Summary

Results are presented on the cross section, differential distributions and charged multiplicity dependence for inclusive Δ^{++} production at 205 GeV/c. Comparison with data at other energies suggests the production cross section is approximately constant for beam momentum >100 GeV/c. We conclude that not all of the Δ^{++} production can be attributed to fragmentation products of diffractively-produced objects. Substantial disagreement is observed between the data and the predictions using an unmodified triple Regge $\pi\pi P + \pi\pi R$ Born term indicating the presence of substantial off-mass-shell or absorptive corrections.

Acknowledgements

Informative discussions with E. Berger and G. C. Fox are acknowledged. We are indebted to T. Akiba for communication of his absorptive triple Regge model calculations. We thank K. Jaeger for providing the data on Λ and $\bar{\Lambda}$ production.

References

1. For a summary of the bubble chamber data, see J. Whitmore, Physics Reports 10C, 273 (1974). A general review was recently given by A.N. Diddens, Proceedings of the XVII International Conference on High Energy Physics, London (1974), p. I-41.

2. P. Capiluppi, et al., Nucl. Phys. B79, 189, (1974) gives a recent summary of the experimental situation.

3. F.T. Dao et al., Phys. Rev. Letters 30, 34 (1973).

4. S.J. Barish et al., Phys. Rev. D9, 2689 (1974).

5. G. Charlton et al., Phys. Rev. Letters 30, 574 (1973); K. Jaeger et al., ANL/HEP 7461, Phys. Rev. D to be published.

6. The complete 2-prong data from this experiment have been published (S.J. Barish et al., Phys. Rev. D9, 1171 (1974)). The complete 4-prong data may be found in Ref. 13.

7. The 12 and 24 GeV/c data come from the Bonn-Hamburg-Munich experiment and were kindly supplied to us by Paul Söding. The 69 GeV/c data are from H. Bialkowska et al., France-Soviet Union collaboration, paper submitted to the XVII International Conference on High Energy Physics, London (1974); the 303 GeV/c data are from Ref. 3, and the 205 GeV/c data are from the present experiment.

8. The cross sections at 102 GeV/c and 400 GeV/c are from data presented by J.P. De Brion et al., University of Rochester report UR-511 (unpublished). They quote cross sections of 1.43 ± 0.10 mb at 102 GeV/c and 1.36 ± 0.14 mb at 400 GeV/c with the selections $|t_{p\Delta}| < 0.6(\mathrm{GeV/c})^2$, $x < -0.7$ and $1.12\ \mathrm{GeV} \leq M(p\pi^+) \leq 1.32$ GeV. For the same selections we obtain a cross section of 1.28 ± 0.08 mb. Since the invariant mass distributions at 102 GeV/c and at 400 GeV/c are very similar to those shown in Fig. 4, we have taken the liberty of scaling the numbers given in this footnote by a ratio obtained from our own data to obtain the cross sections shown dotted in Fig. 5.

9. T. Kasahara and T. Akiba, Prog. of Theoretical Physics 51, 1473 (1974). We are grateful to these authors for communication of their calculations.

10. S.J. Barish et al., Phys. Rev. Letters 31, 1080 (1973); see also Ref. 1 for more details.

11. J. Whitmore and M. Derrick, Phys. Letters 50B, 280 (1974).

12. D. Brick et al., Phys. Rev. Letters 31, 488 (1973).

13. M. Derrick et al., Phys. Rev. D9, 1853 (1974).

14. P. Schultz et al., ANL/HEP 7428, paper submitted to the XVII International Conference on High Energy Physics, London (July 1974).

15. E. Gotsman, Phys. Rev. D9, 1575 (1974).

16. M. Bishari, Phys. Rev. Letters 38B, 510 (1972).

17. J. Pumplin, Phys. Rev. D8, 2249 (1973).

18. R. D. Field and G. C. Fox, Nucl. Phys. B80, 367 (1974).

19. At fixed t the $\pi\pi\mathbb{P}$ contribution to $d\sigma/dtdx$ behaves like $(1 - |x|)^{1-2\alpha_\pi(t)}$ and hence increases as $|x|$ decreases. The turn over and decrease in the predicted $\pi\pi P$ contributions shown in Fig. 14(b) and Fig. 16 is due to the fact that the experimental data are not at fixed t due to t_{min} effects. As $|x|$ decreases $|t_{min}|$ increases and since the $\pi\pi\mathbb{P}$ term is sharply peaked in t this effect overcomes the rise due to the $|x|$ dependence resulting in a net decrease.

Figure Captions

Fig. 1 P_T^2 versus x for the inclusive reactions p + p → p + Anything and p + p → π + Anything at 205 GeV/c for $P_{Lab} \leq 1.4$ GeV/c; the dotted line corresponds to the reaction p + p → Δ^{++} + Anything for $|t_{p\Delta}| = 1.0$ $(GeV/c)^2$. The data of the experiment are shown as the dots.

Fig. 2 The invariant mass distribution for (a) all $p\pi^+$ and (b) all $p\pi^-$ combinations in events with a proton and one or more pions having $P_{Lab} \leq 1.4$ GeV/c. The shaded histogram in each case is obtained by requiring $|t_{p\Delta}| \leq 1.0$ $(GeV/c)^2$.

Fig. 3 The invariant mass distribution for all $p\pi^+$ combinations with $|t_{p,(p\pi^+)}| \leq (1$ $GeV/c)^2$ shown for different event topologies. The weighted events are used; events having $M(p\pi^+) > 1.8$ GeV are lumped in one bin above the dotted line.

Fig. 4 The normalized $p\pi^+$ invariant mass distribution for p + p → p + π^+ + X^0 at 12, 24, 69, 205 and 303 GeV/c. In each case, the selection $|t_{p,(p\pi^+)}| \leq 1.0$ $(GeV/c)^2$ has been made. The same background curve is drawn for each energy.

Fig. 5 The production cross section for the inclusive process p + p → $\Delta^{++}(1236)$ + X^0 as a function of incident beam momentum. Ref. 8 explains how the 102 GeV/c and 400 GeV/c values were obtained.

Fig. 6(a) The invariant mass of the $p\pi^+\pi^-$ system where all three particles have laboratory momentum $\leq$ 1.4 GeV/c. In (b) the further selection of $p\pi^+$ mass in the $\Delta^{++}(1236)$ region is imposed; (c) the $\pi^+\pi^-$ invariant mass distribution corresponding to the data in (a).

Fig. 7 Diagrams appliable to (a) the diffractive proton reaction, (b) a triple-Regge-model of the inclusive proton reaction, (c) the inclusive Δ^{++} reaction and (d) a triple-Regge-model of the inclusive Δ^{++} reaction.

Fig. 8 The missing-mass squared distribution for the inclusive proton (scale on right) and inclusive Δ^{++} reactions (scale on left) at 205 GeV/c. The microbarn equivalent is 4.35 ± 0.1 μb/event in the former case and 4.66 μb/event in the latter. No peak at low M^2 is seen for the Δ^{++} reaction above the hand drawn curve.

Fig. 9 The mean charged multiplicity of the system X at equivalent center of mass energies in (a) $p + p \rightarrow \Delta^{++} + X^o$ data and a curve showing the on-shell $\pi^- p \rightarrow X^o$, and (b) a similar comparison between the reactions $p + p \rightarrow$ "Δ^o" $+ X^{++}$ and $\pi^+ p \rightarrow X^{++}$.

Fig. 10 The average charged multiplicity, $\langle n_c \rangle$, as a function of Feynman x for inclusive p, Λ^o, π^-, K_s^o, Δ^{++} and "Δ^o" production

in pp interactions at 19 GeV/c and 205 GeV/c. The 19 GeV/c data comes from H. Boggild et al., Nucl. Phys. B72, 221 (1974).

Fig. 11 The normalized charged multiplicity distributions at 205 GeV/c for the processes (a) $p + p \rightarrow$ Anything, (b) $p + p \rightarrow \Delta^{++}$ + Anything, (c) $p + p \rightarrow$ diffractive production of low mass states. The distribution for events with a Δ^{++} is broader than the multiplicity distribution for the diffractive events but narrower than the overall multiplicity distribution.

Fig. 12 The CM rapidity (y^*) distribution for the inclusive processes (a) $p + p \rightarrow p + X^+$ (b) $p + p \rightarrow p + X^+$ with $M_X^2 \geq 40$ GeV^2, (c) $p + p \rightarrow \Delta^{++} + X^o$, (d) $p + p \rightarrow p + \geq 1$ slow $\pi^\pm + X^o$, and (e) $p + p \rightarrow \Lambda^o (\bar{\Lambda}^o) + X^{++}$.

Fig. 13 The P_T^2 distribution for the reactions $p + p \rightarrow p + \geq 1$ slow $\pi^\pm + X^o$, $p + p \rightarrow \Lambda^o + X^{++}$ and $p + p \rightarrow \Delta^{++} + X^o$.

Fig. 14 The $t' (= t - t_{min})$ distribution for the reaction $p + p \rightarrow \Delta^{++} + X^o$.

Fig. 15 The Feynman x distribution for the reaction $p + p \rightarrow \Delta^{++} + X^o$ with (a) $|t_{p\Delta}| \leq 1.0$ (GeV/c)^2 and (b) with the additional selection $P_T^2 \leq 0.1$ (GeV/c)^2. In (b) the total OPE Born term calculation is shown together with the sum of the ($\rho\rho\mathbb{P}$ and $A_2A_2\mathbb{P}$) contributions.

Fig. 16 The Feynman x distribution for $p + p \rightarrow \Delta^{++} + X^o$ compared to the

Born OPE calculation multiplied by exp (6t) and added to the sum of the ($\rho\rho\mathbb{P}$ and $A_2A_2\mathbb{P}$) contributions. In all cases the selections $|t_{p\Delta}| \leq 1.0$ (GeV/c)^2 and $P_T^2 \leq 0.1$ (GeV/c)^2 have been made.

Fig. 17 The distributions in the polar and azimuthal angles for the Δ decay in the Gottfried-Jackson reference frame (a, b) for $\Delta^{++} \rightarrow p\pi^+$ and (c, d) for $\Delta^0 \rightarrow p\pi^-$. In all the cases the selections $|t_{p\Delta}| \leq 1.0$ (GeV/c)^2 and $P_T^2 \leq 0.1$ (GeV/c)^2 have been made. The Δ is defined by the mass selection $1.12 \leq$ Mass $(p\pi) \leq 1.32$ GeV.

Table I

Multiplicity Distributions of Events With Low Momentum Particles

Prong Number	2	4	6	8	10	12	14	16	18	20
Events With Proton and $\leq 1\,\pi$ Identified ($P_{Lab} \leq 1.4$ GeV/c)	7	292	295	228	169	75	25	12	3	2
Weighted Events[a]	7.5	311.3	331.3	228.0	161.6	77.6	23.6	11.2	2.8	1.9
Number of the Above With $\leq 1\Delta^{++}$ and with $\lvert t_{2p\Delta} \rvert \leq 1.0$ (GeV/c)^2	6.4	129.0	140.4	81.0	45.2	23.1	4.9	2.8	0.0	0.9

[a] The weight is defined to be 1.0 for the 8 prong events. The weighted events correspond to a normalization of 4.66 μb/event.

Table II

Charge Distribution of Slow π's ($P_{lab} < 1.4$ GeV/c) For Events With a Slow Proton

		Number of π^-'s					Totals	
		0	1	2	3	4	205 GeV/c	303 GeV/c[a]
Number of π^+'s	0	-	201	27	3	0	231	-
	1	369	296	56	4	2	727	166
	2	56	48	21	4	1	130	41
	3	4	7	3	2	0	16	7
	4	0	0	1	0	0	1	
205 GeV/c Totals		429	552	108	13	3		
303 GeV/c[a] Totals			150	32	3			

[a] Ref. 3

Table III

The Δ^{++} and Δ^{o} Inclusive Cross Sections

Method	$\sigma(\Delta^{++})$ mb	$\sigma(\Delta^{o})$ mb ($n\pi^{o}$ mode included)
Background Subtracted Mass $(p\pi^{+}) \leq 1.5$ GeV	1.30 ± 0.14	0.33 ± 0.36
Mass Slice $1.12 \leq$ Mass $(p\pi^{+}) \leq 1.32$ GeV	2.02 ± 0.10	

Table IV

Single Hemisphere Diffractive and Δ^{++} Cross Sections

Topology	σ (Diffractive) mb [a]	$\sigma(\Delta^{++})$ mb for $\lvert t_{p\Delta^{++}} \rvert \leq 1 (\mathrm{GeV}/c)^2$
2	1.13 ± 0.10	0.024 ± 0.011
4	1.28 ± 0.08	0.46 ± 0.07
6	0.36 ± 0.08	0.49 ± 0.08
8	0.02 ± 0.01	0.17 ± 0.07
≥ 10	0	0.16 ± 0.08

(a) From Ref. 4

Table V

Density Matrix Elements for $\Delta^{++} \rightarrow p + \pi^+$ in the Reaction $p + p \rightarrow \Delta^{++} + X^o$

Cuts	ρ_{11}	Re ρ_{31}	Re ρ_{3-1}
$1.12 \leq$ Mass $(p\pi^+) \leq 1.32$ GeV $\lvert t_{p\Delta} \rvert \leq 1.0$ (GeV/c)^2; $P_T^2 \leq 0.1$ (GeV/c)^2	0.39 ± 0.04	0.01 ± 0.04	0.02 ± 0.04

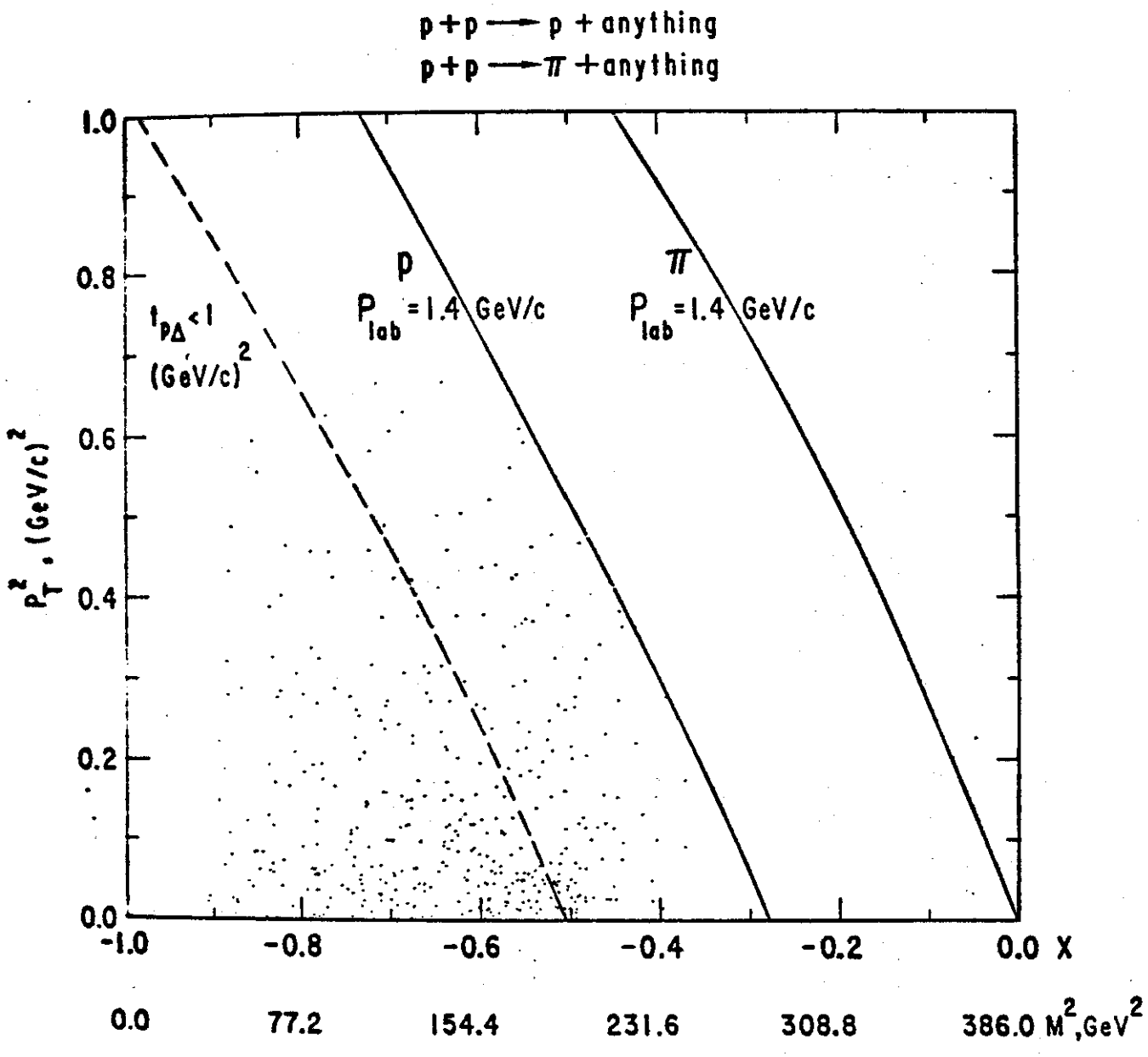
p+p ⟶ p + anything
p+p ⟶ π +anything
1.0
0.8
0.6
0.4
0.2
0.0
p_T^2 , $(GeV/c)^2$
$t_{p\Delta} < 1$
$(GeV/c)^2$
p
P_{lab} = 1.4 GeV/c
π
P_{lab} = 1.4 GeV/c
-1.0
-0.8
-0.6
-0.4
-0.2
0.0 X
0.0
77.2
154.4
231.6
308.8
386.0 M^2,GeV^2

Figure 1

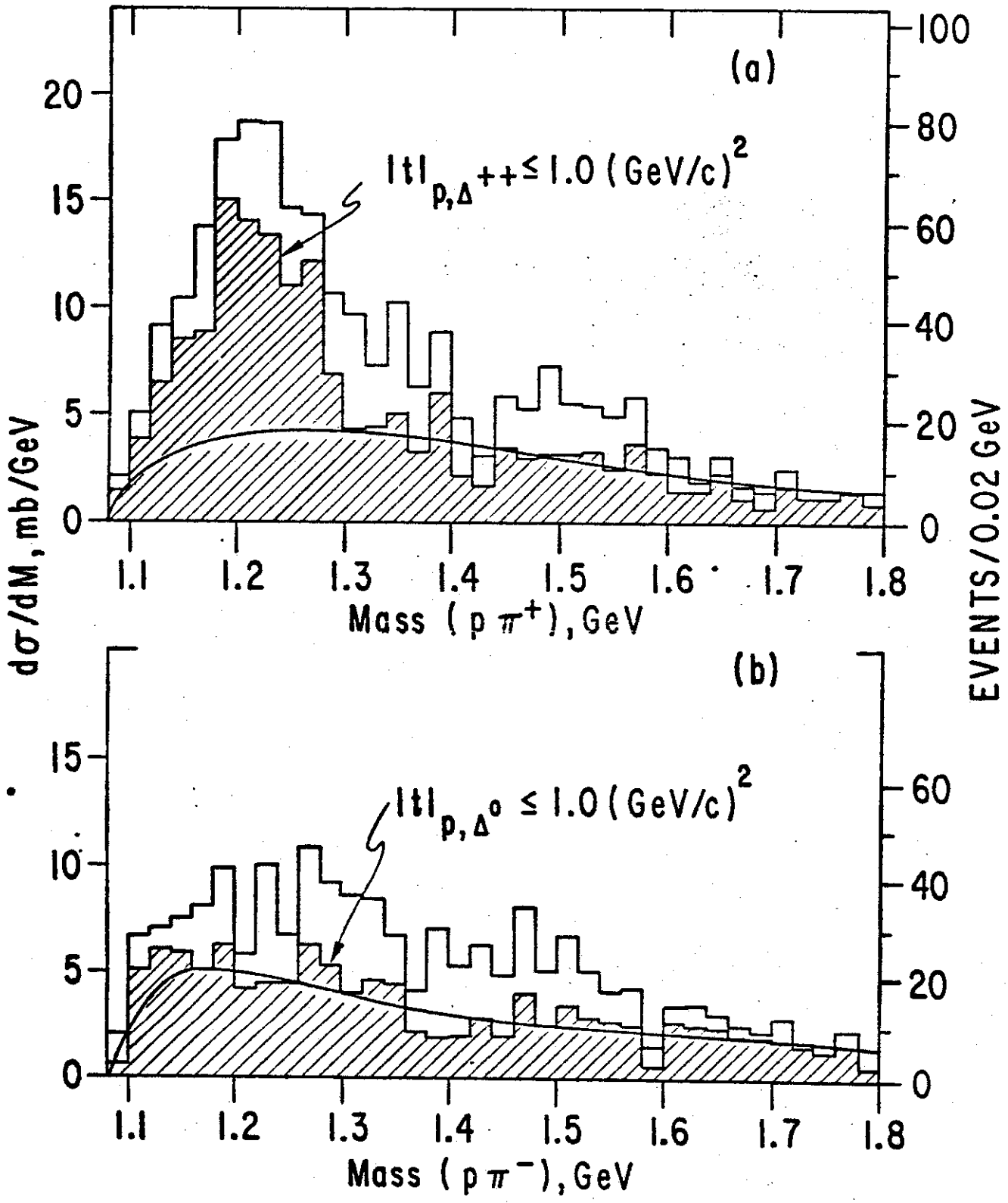
(a)
$|t|_{p,\Delta^{++}} \leq 1.0\ (GeV/c)^2$
$d\sigma/dM$, mb/GeV
EVENTS/0.02 GeV
Mass $(p\pi^+)$, GeV
(b)
$|t|_{p,\Delta^0} \leq 1.0\ (GeV/c)^2$
Mass $(p\pi^-)$, GeV

Figure 2

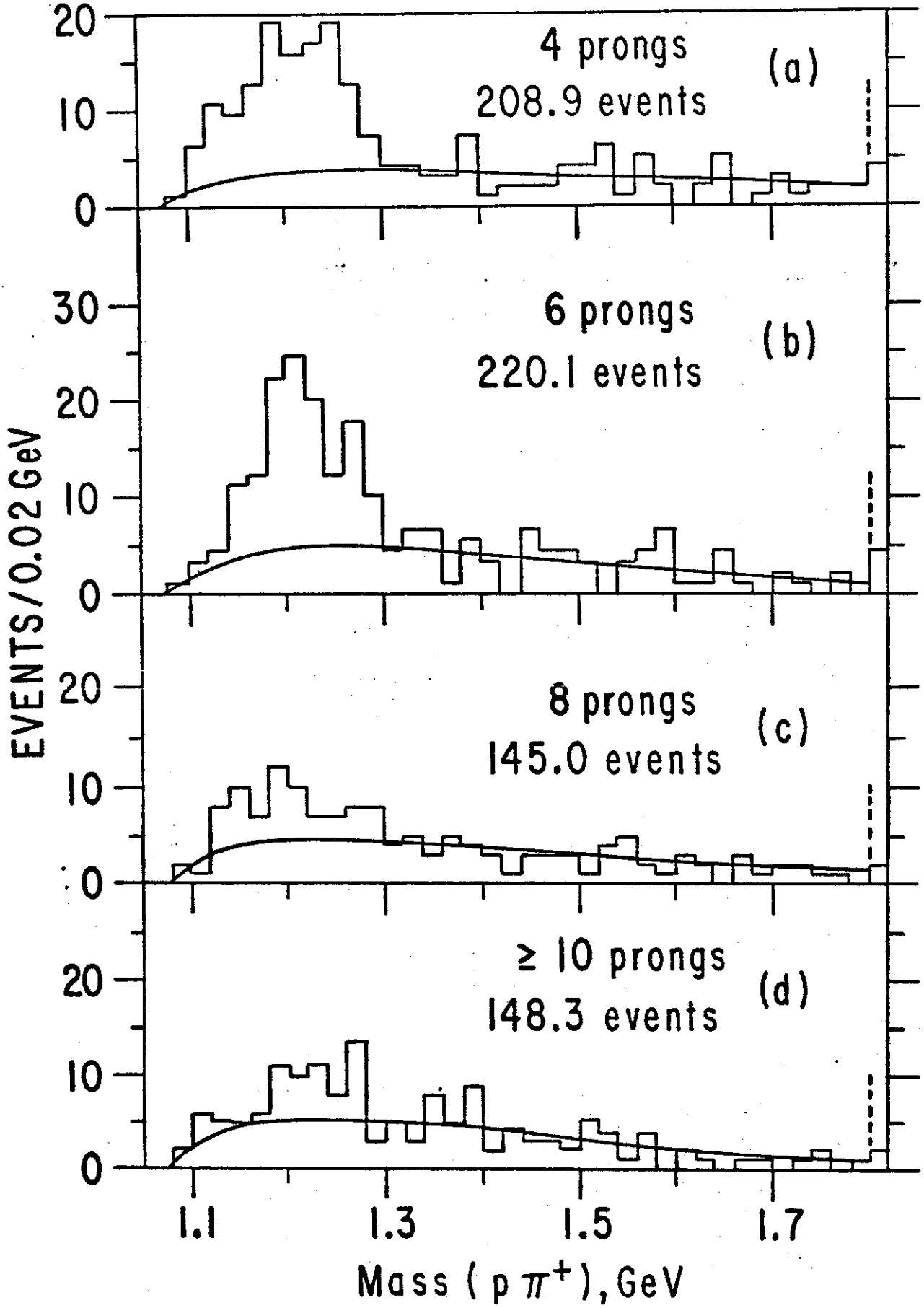
4 prongs
208.9 events
(a)
6 prongs
220.1 events
(b)
8 prongs
145.0 events
(c)
≥ 10 prongs
148.3 events
(d)
EVENTS/0.02 GeV
Mass (p π+), GeV
1.1
1.3
1.5
1.7

Figure 3

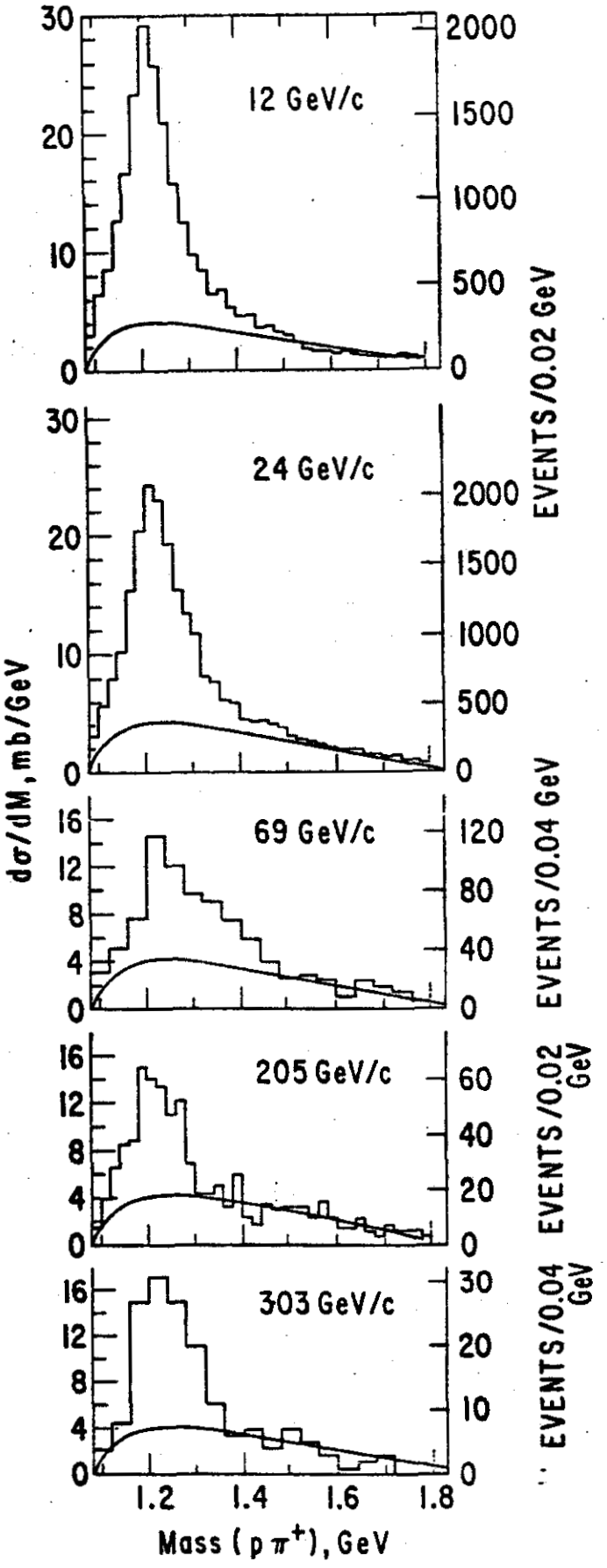
12 GeV/c
24 GeV/c
69 GeV/c
205 GeV/c
303 GeV/c
dσ/dM, mb/GeV
EVENTS/0.02 GeV
EVENTS/0.04 GeV
EVENTS/0.02 GeV
EVENTS/0.04 GeV
Mass (p π+), GeV

Figure 4

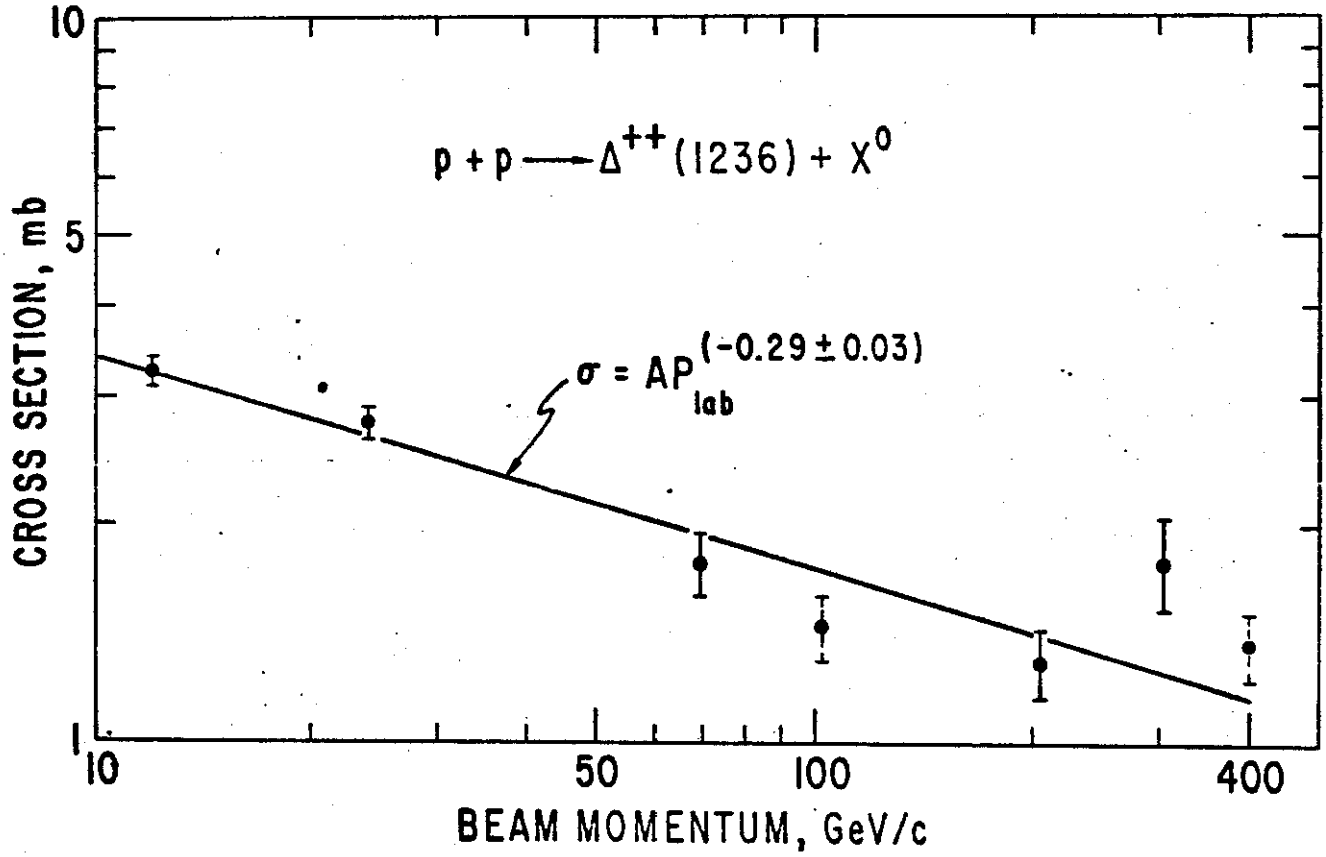
10
5
1
CROSS SECTION, mb
p + p ⟶ Δ++ (1236) + X0
σ = AP lab (-0.29 ± 0.03)
10
50
100
400
BEAM MOMENTUM, GeV/c

Figure 5

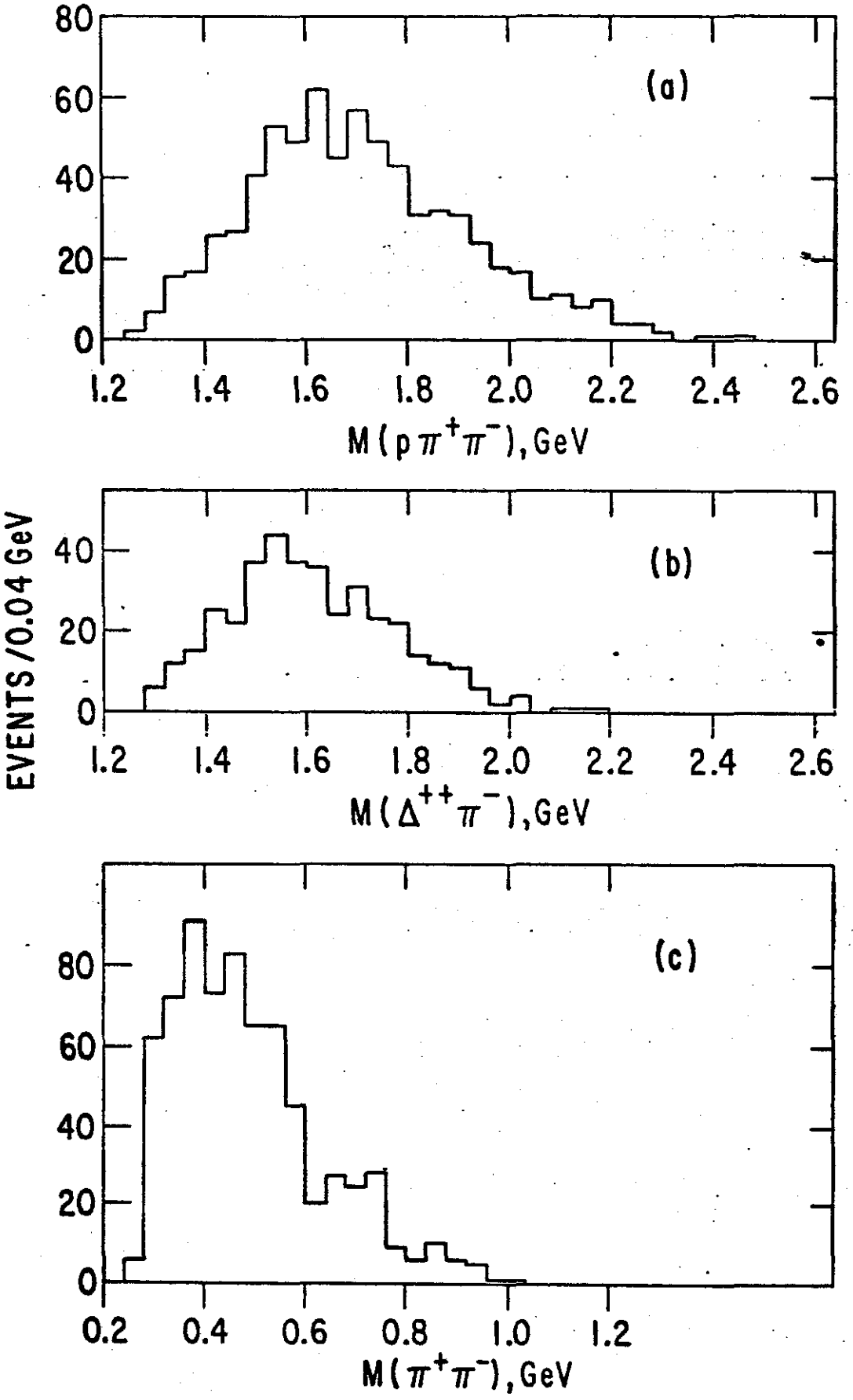
(a)
80
60
40
20
0
1.2
1.4
1.6
1.8
2.0
2.2
2.4
2.6
M(pπ⁺π⁻), GeV
EVENTS/0.04 GeV
(b)
40
20
0
M(Δ⁺⁺π⁻), GeV
(c)
0.2
0.4
0.6
0.8
1.0
1.2
M(π⁺π⁻), GeV

Figure 6

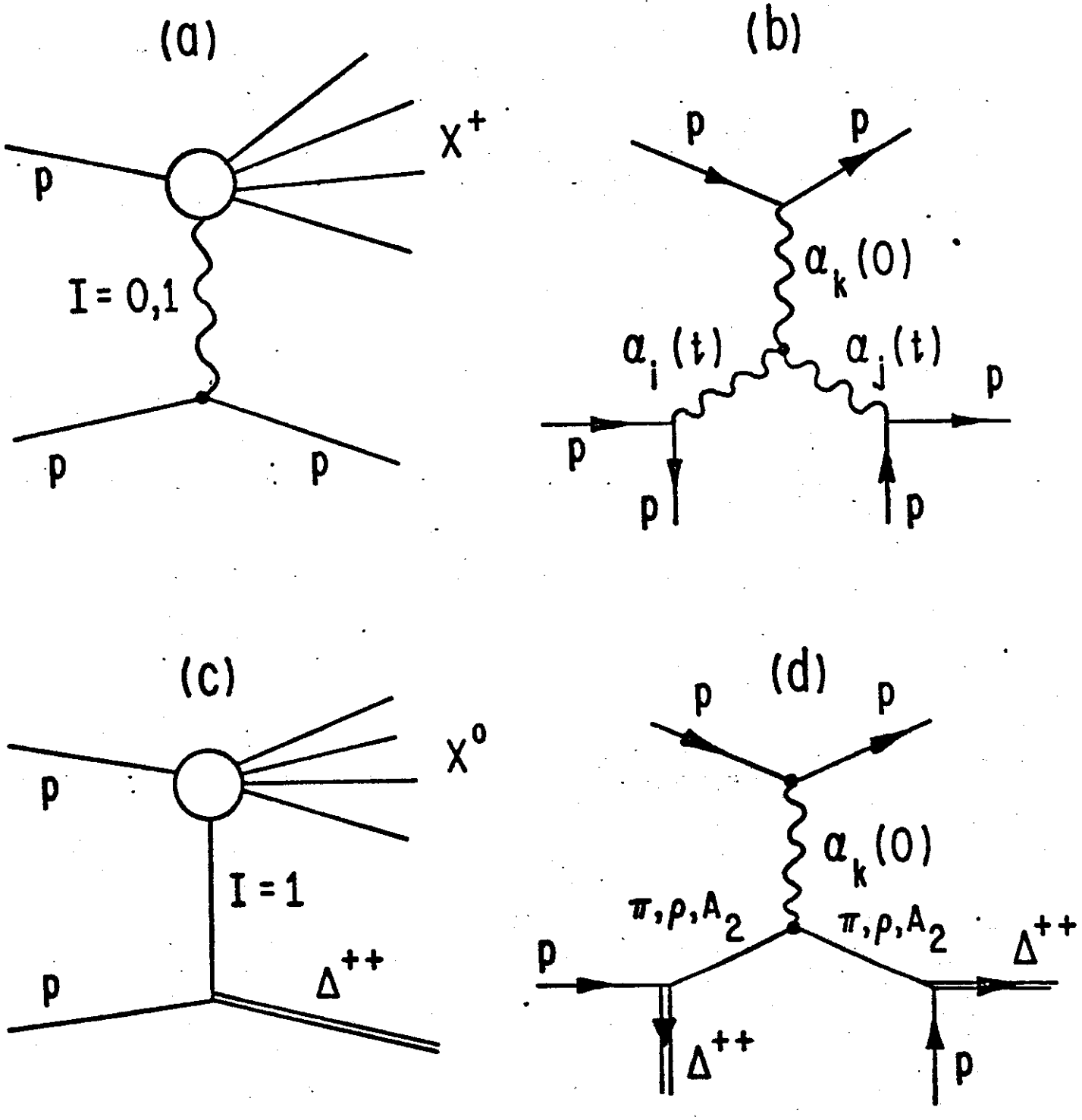
(a)
p
X+
I = 0,1
p
p
(b)
p
p
αk(0)
αi(t)
αj(t)
p
p
p
p
(c)
p
X0
I = 1
p
Δ++
(d)
p
p
αk(0)
π,ρ,A2
π,ρ,A2
Δ++
p
Δ++
p

Figure 7

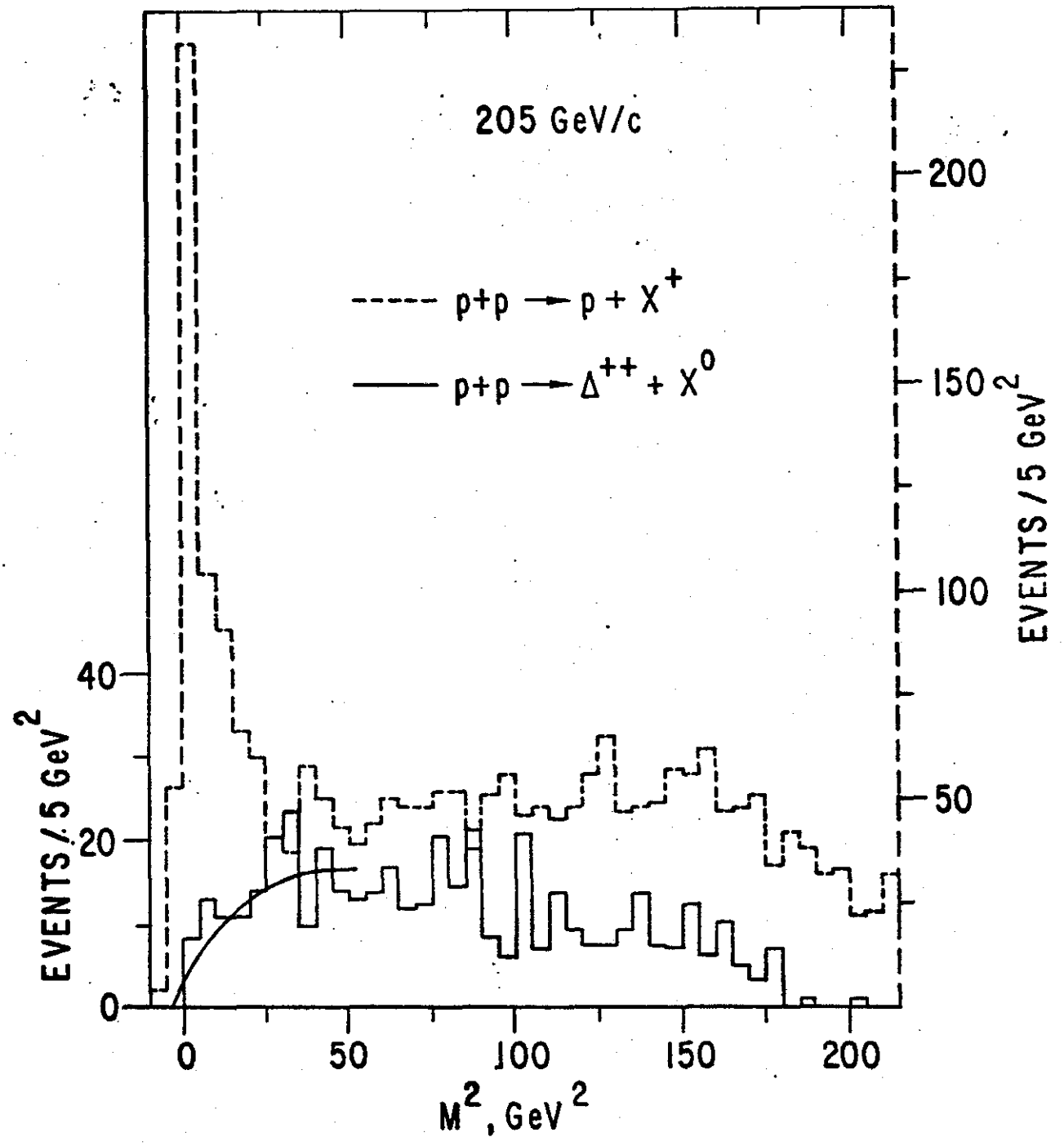
205 GeV/c
p+p → p + X+
p+p → Δ++ + X0
EVENTS/5 GeV2
EVENTS/5 GeV2
M2, GeV2
0
20
40
50
100
150
200

Figure 8

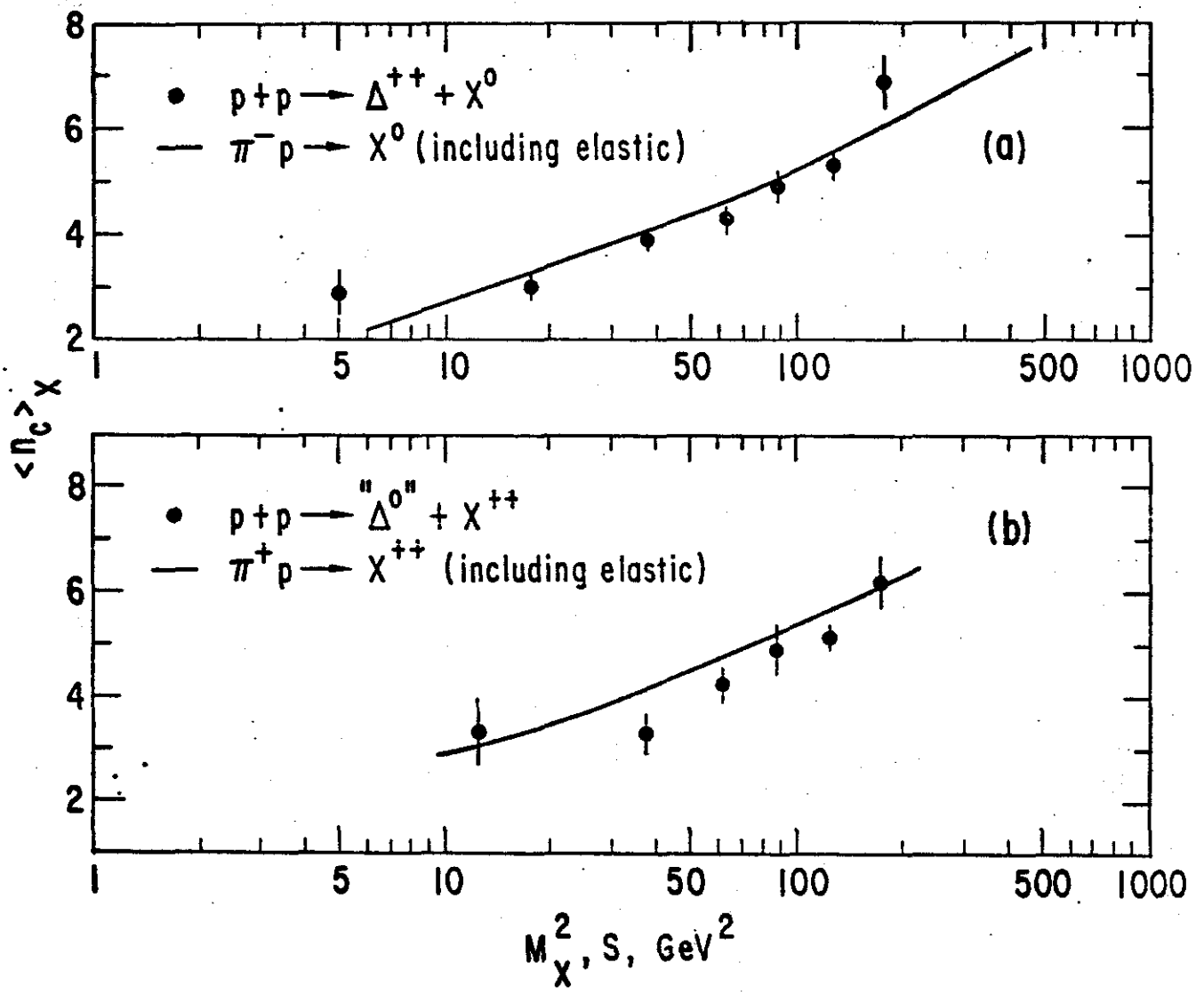
8
6
4
2
p + p → Δ++ + X0
π− p → X0 (including elastic)
(a)
1
5
10
50
100
500
1000
<nc>X
p + p → "Δ0" + X++
π+ p → X++ (including elastic)
(b)
M2X, S, GeV2

Figure 9

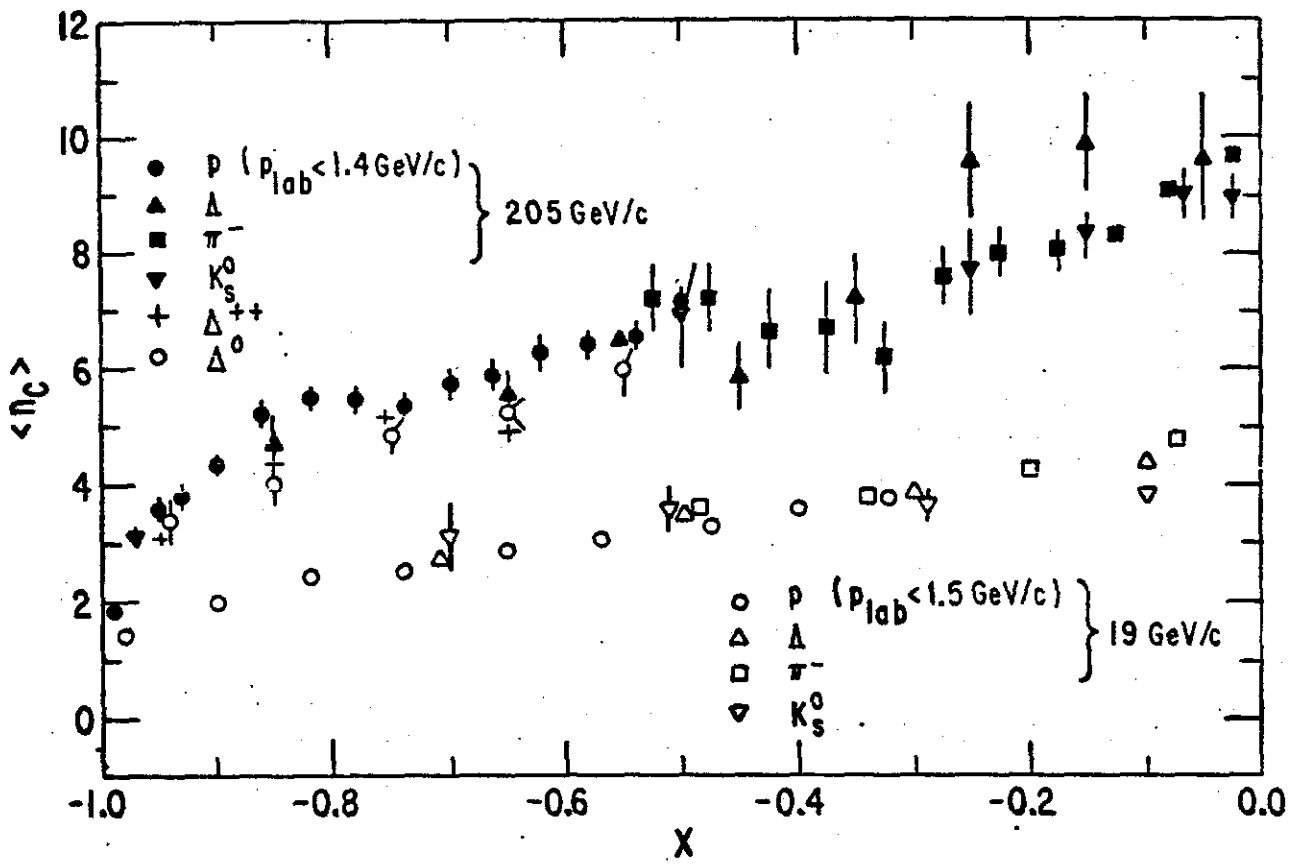
12
10
8
6
4
2
0
-1.0
-0.8
-0.6
-0.4
-0.2
0.0
X
<nc>
p (p_lab<1.4 GeV/c)
Λ
π⁻
K⁰s
Δ⁺⁺
Δ⁰
205 GeV/c
p (p_lab<1.5 GeV/c)
Λ
π⁻
K⁰s
19 GeV/c

Figure 10

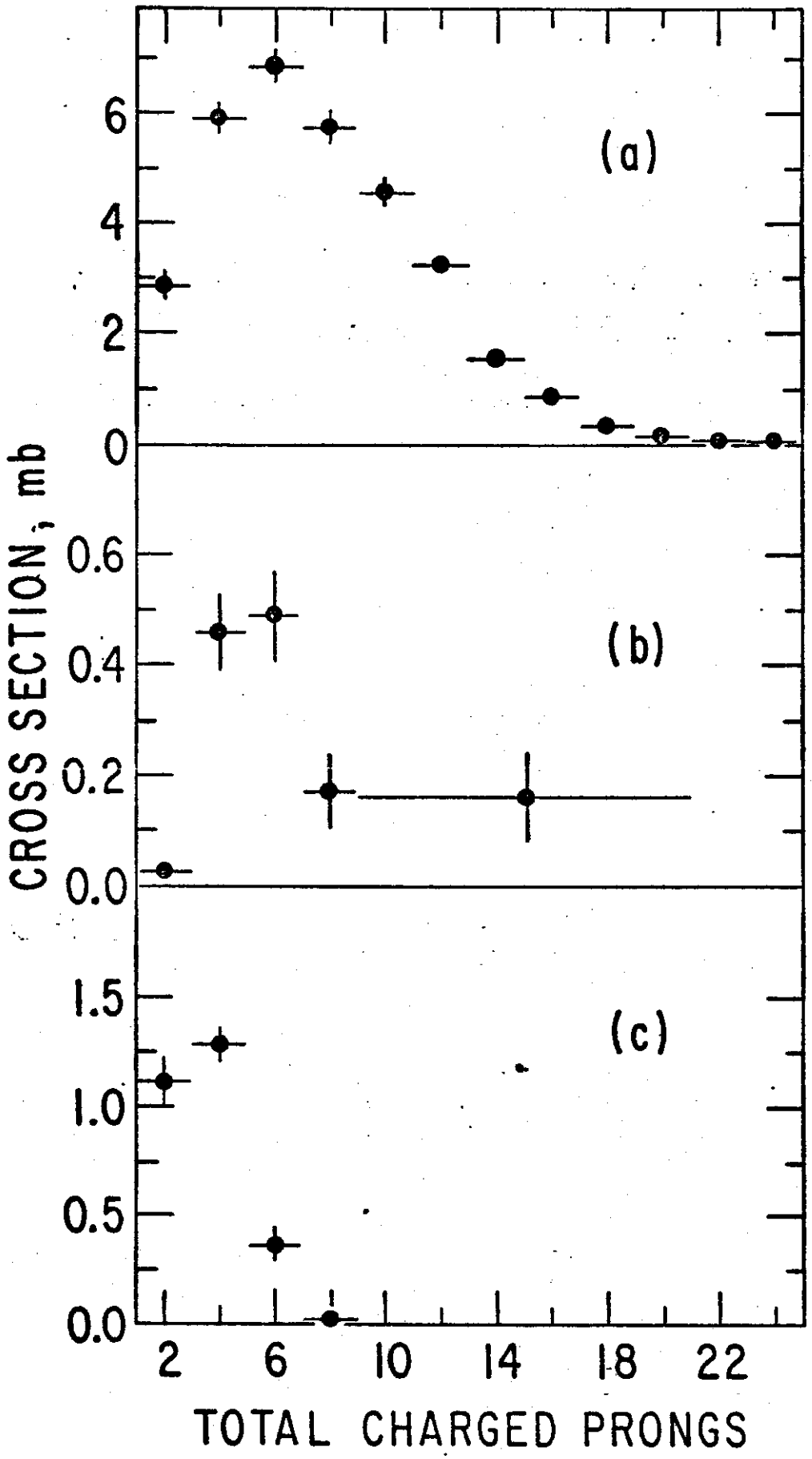
CROSS SECTION, mb
(a)
(b)
(c)
6
4
2
0
0.6
0.4
0.2
0.0
1.5
1.0
0.5
0.0
2
6
10
14
18
22
TOTAL CHARGED PRONGS

Figure 11

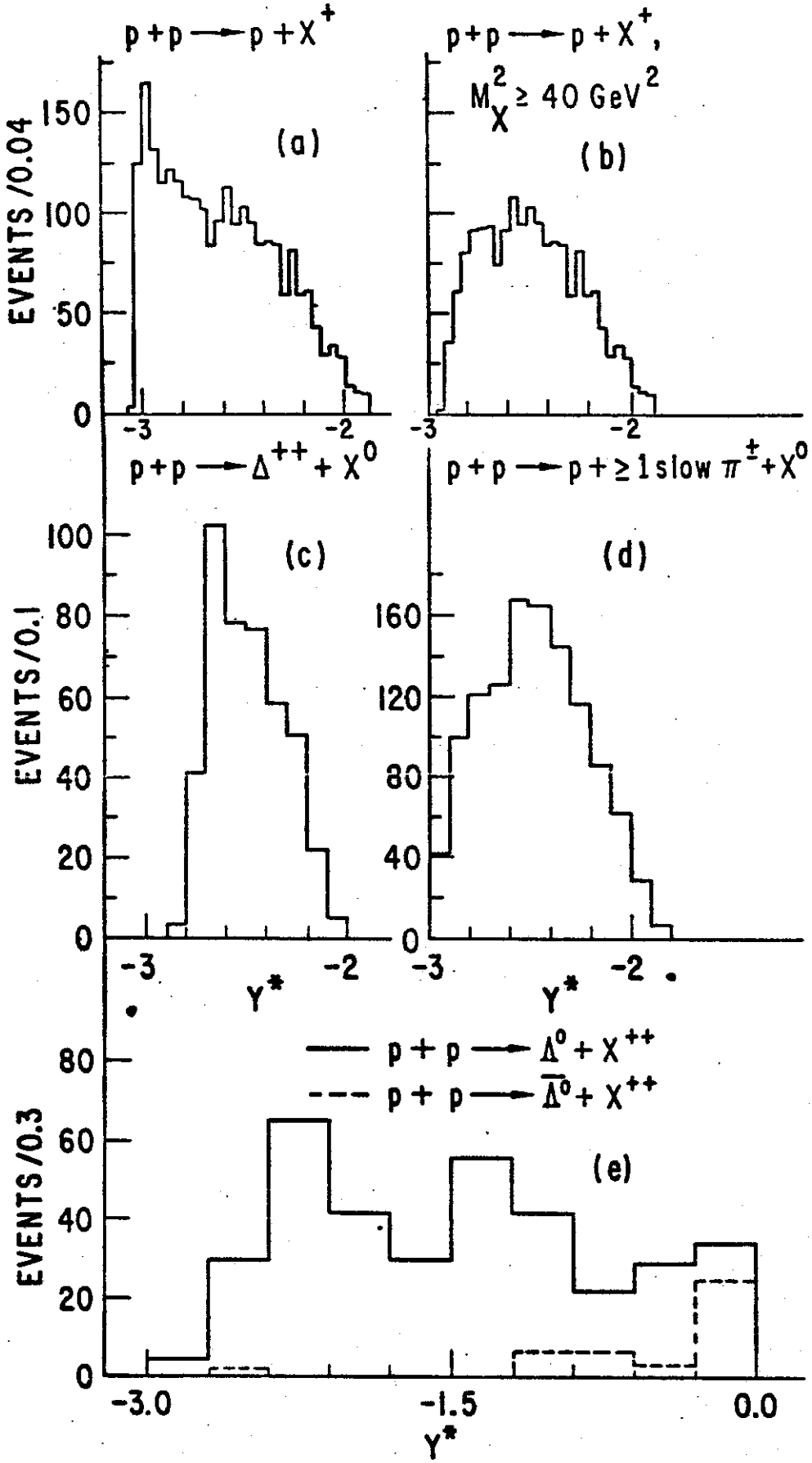
p + p → p + X+
(a)
EVENTS /0.04
150
100
50
0
-3
-2
p + p → p + X+,
M2X ≥ 40 GeV2
(b)
p + p → Δ++ + X0
(c)
EVENTS/0.1
100
80
60
40
20
0
Y*
p + p → p + ≥1 slow π± + X0
(d)
160
120
80
40
p + p → Λ0 + X++
p + p → Λ̄0 + X++
(e)
EVENTS/0.3
-3.0
-1.5
0.0

Figure 12

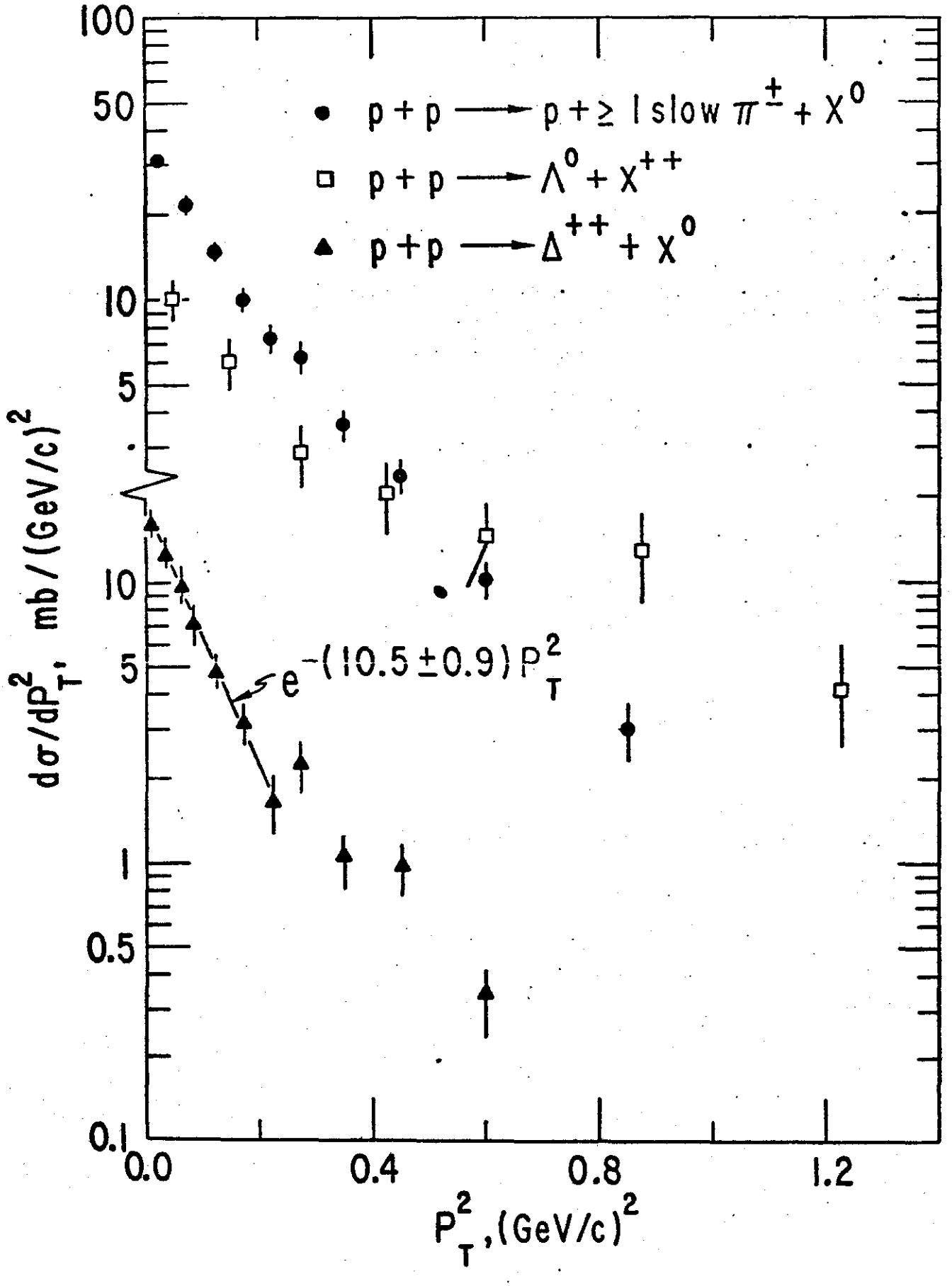
100
50
10
5
10
5
1
0.5
0.1
0.0
0.4
0.8
1.2
p + p → p + ≥ 1 slow π± + X0
p + p → Λ0 + X++
p + p → Δ++ + X0
e-(10.5 ±0.9) P2T
dσ/dP2T, mb/(GeV/c)2
P2T, (GeV/c)2

Figure 13

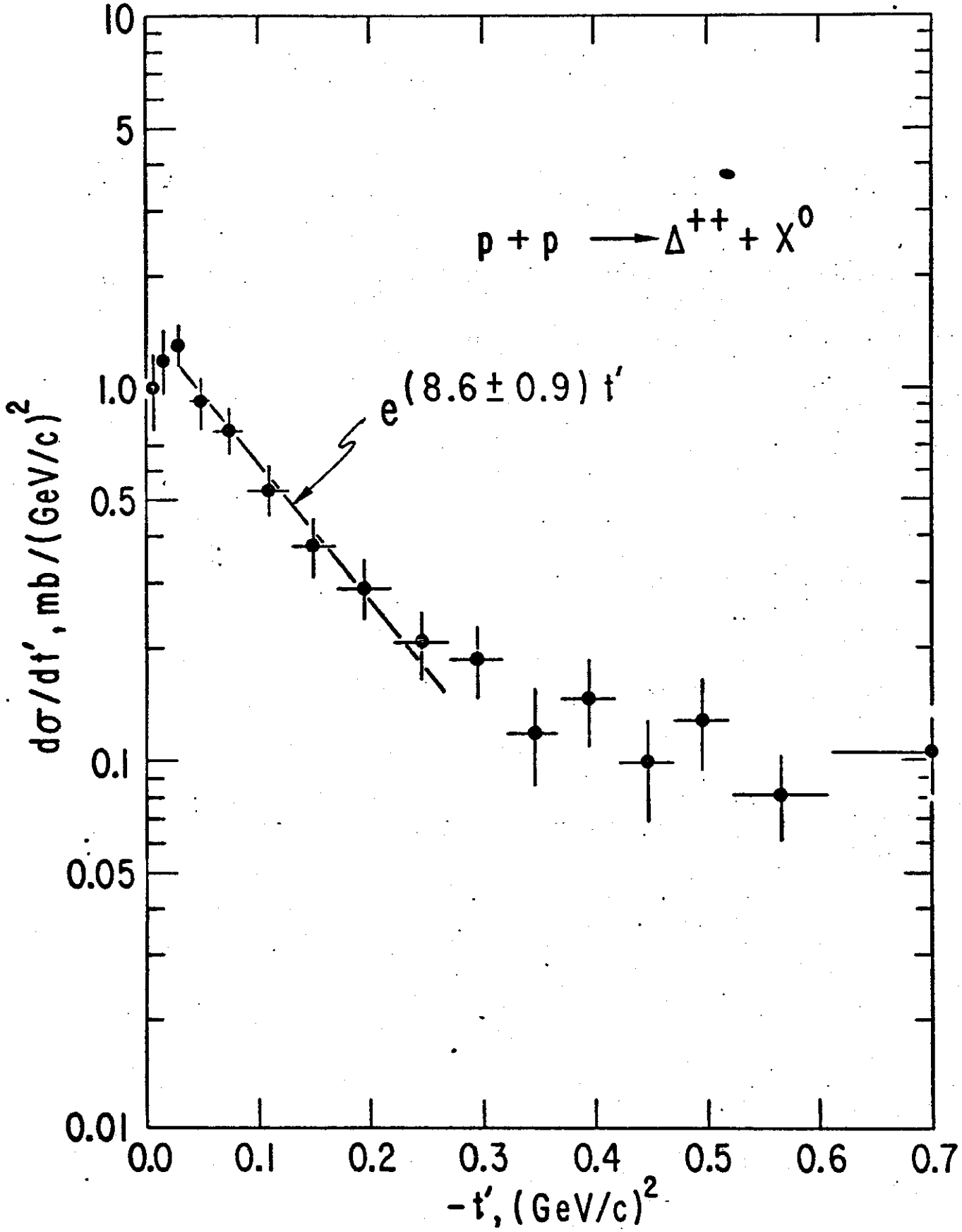
10
5
1.0
0.5
0.1
0.05
0.01
0.0
0.1
0.2
0.3
0.4
0.5
0.6
0.7
p + p → Δ++ + X0
e(8.6 ± 0.9) t'
dσ/dt', mb/(GeV/c)2
-t', (GeV/c)2

Figure 14

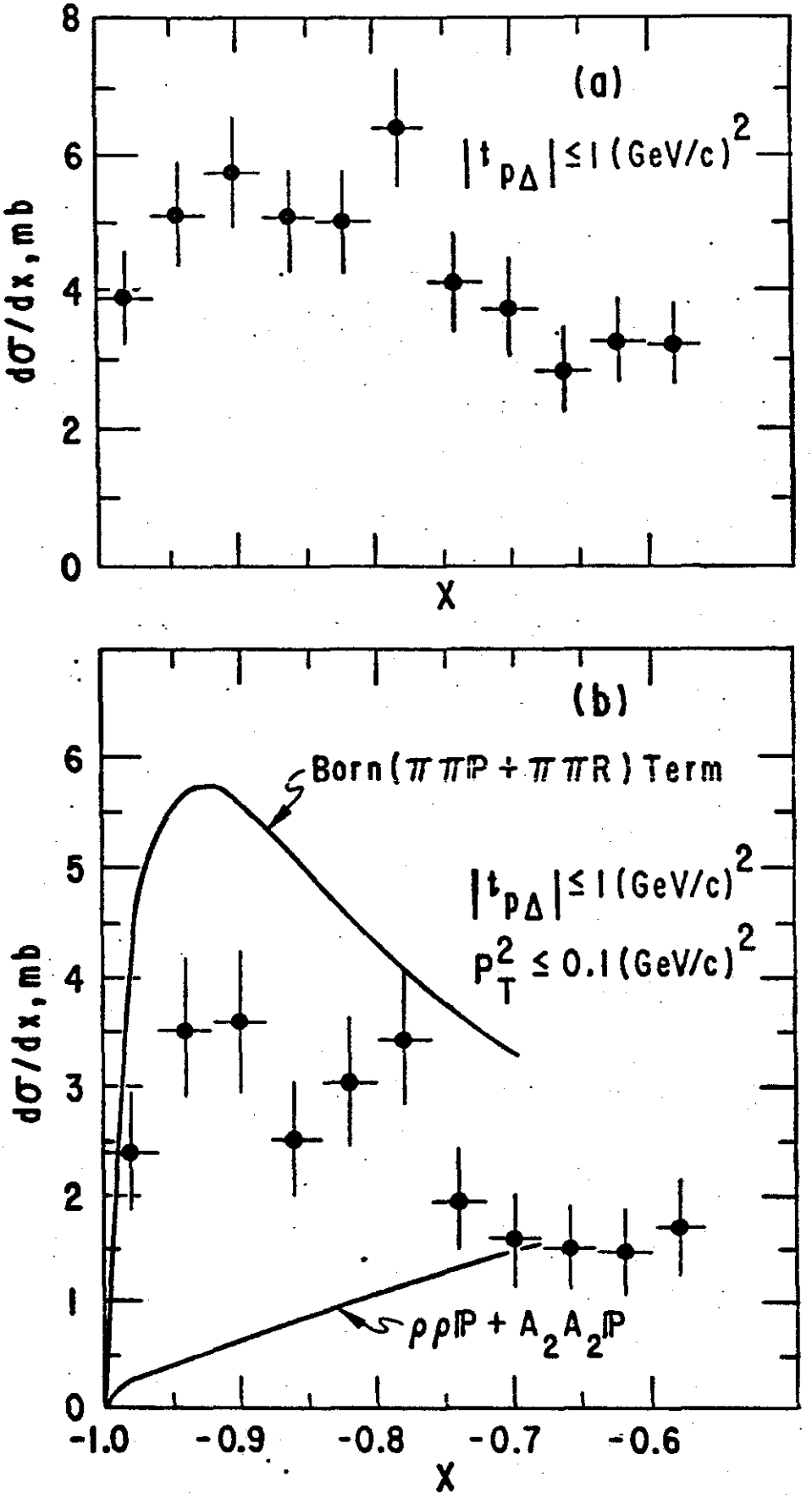
(a)
$|t_{p\Delta}| \leq 1\ (GeV/c)^2$
dσ/dx, mb
X
(b)
Born ($\pi\pi\mathbb{P} + \pi\pi R$) Term
$|t_{p\Delta}| \leq 1\ (GeV/c)^2$
$p_T^2 \leq 0.1\ (GeV/c)^2$
$\rho\rho\mathbb{P} + A_2A_2\mathbb{P}$
dσ/dx, mb
X
-1.0
-0.9
-0.8
-0.7
-0.6

Figure 15

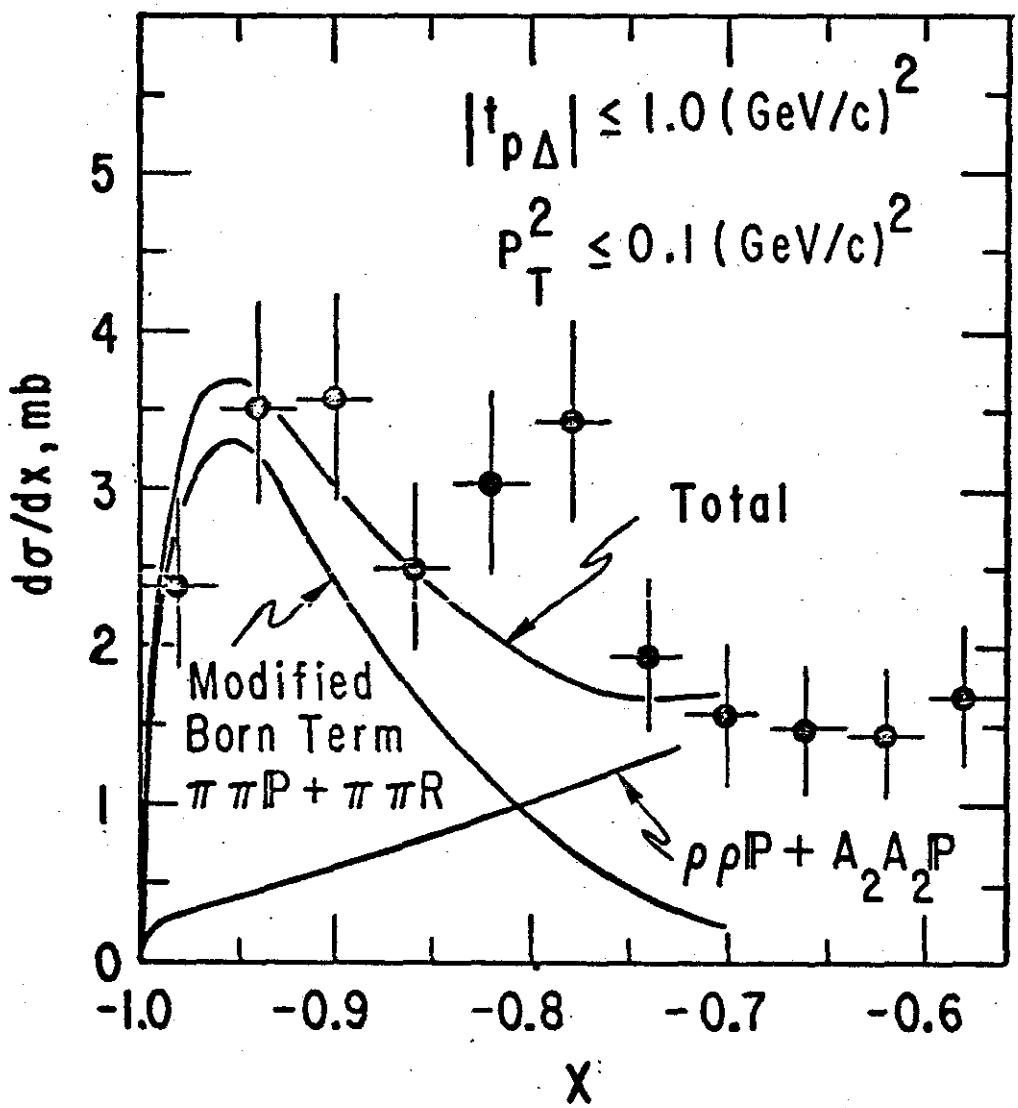
$|t_{p\Delta}| \leq 1.0\ (GeV/c)^2$
$P_T^2 \leq 0.1\ (GeV/c)^2$
Total
Modified
Born Term
$\pi\pi\mathbb{P} + \pi\pi R$
$\rho\rho\mathbb{P} + A_2A_2\mathbb{P}$
$d\sigma/dx$, mb
X
0
1
2
3
4
5
-1.0
-0.9
-0.8
-0.7
-0.6

Figure 16

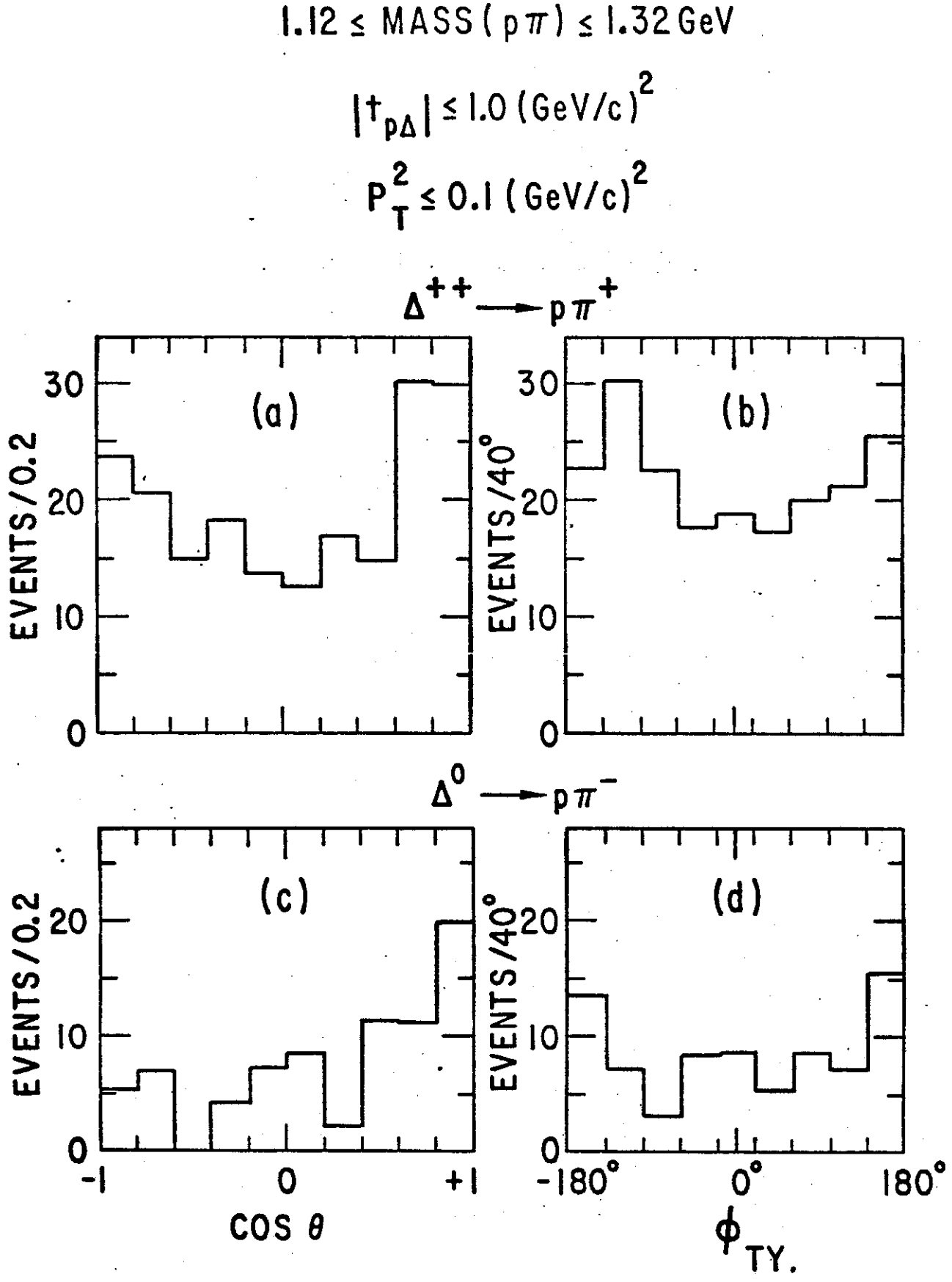
1.12 ≤ MASS (pπ) ≤ 1.32 GeV
|t_pΔ| ≤ 1.0 (GeV/c)²
P_T² ≤ 0.1 (GeV/c)²
Δ++ → pπ+
Δ0 → pπ−
(a)
(b)
(c)
(d)
EVENTS/0.2
EVENTS/40°
COS θ
φ TY.
-1
0
+1
-180°
0°
180°

Figure 17